

# Journal of Materials Chemistry A

Accepted Manuscript



This is an *Accepted Manuscript*, which has been through the Royal Society of Chemistry peer review process and has been accepted for publication.

*Accepted Manuscripts* are published online shortly after acceptance, before technical editing, formatting and proof reading. Using this free service, authors can make their results available to the community, in citable form, before we publish the edited article. We will replace this *Accepted Manuscript* with the edited and formatted *Advance Article* as soon as it is available.

You can find more information about *Accepted Manuscripts* in the [Information for Authors](#).

Please note that technical editing may introduce minor changes to the text and/or graphics, which may alter content. The journal's standard [Terms & Conditions](#) and the [Ethical guidelines](#) still apply. In no event shall the Royal Society of Chemistry be held responsible for any errors or omissions in this *Accepted Manuscript* or any consequences arising from the use of any information it contains.

## COMMUNICATION

## Enhanced Electrochemical Capabilities of Lithium Ion Batteries by Structurally Ideal Anodic Aluminum Oxide Separator

Cite this: DOI: 10.1039/x0xx00000x

Yong-keon Ahn,<sup>a</sup> Junwoo Park,<sup>a</sup> Dalwoo Shin,<sup>b</sup> Sanghun Cho,<sup>a</sup> Si Yun Park,<sup>a</sup> Hyunjin Kim,<sup>a</sup> Jeeyoung Yoo,<sup>\*a</sup> and Youn Sang Kim<sup>\*a,c</sup>Received 00th January 2015,  
Accepted 00th January 2015

DOI: 10.1039/x0xx00000x

www.rsc.org/

In this study, a novel inorganic separator, porous anodic aluminum oxide (AAO) is introduced for a rechargeable lithium ion battery system. The porous AAO gives rise to an ideal structure for battery separators such as highly ordered pore array, appropriate porosity (67.4 %), extremely low tortuosity, and thermal durability. The prepared AAO separator has average pore sizes of 75 nm and thickness of 54 micrometers, which leads to enhanced ionic conductivity (2.196 mS cm<sup>-1</sup>), discharging capacity at high current rates (20.13 mAh g<sup>-1</sup> at 10 C), and capacity retention (82.9 %). Moreover, the computer simulation (COMSOL) model shows that the ideal AAO separator structure induces stable LIB operation in wide ranges of the current rate, due to effective suppression of Li dendrite formation. AAO separator has a strong potential in massive energy storage systems such as energy storage systems (EES) and electric vehicles (EVs).

Greenhouse gas emission and fossil fuel shortage are growing environmental concerns where energy storage devices are essentially required for efficient energy consumption<sup>1-5</sup>. In particular, Lithium Ion Batteries (LIBs) have flourished due to the needs for huge energy storage systems (ESS) and electric vehicles (EVs) where LIBs are utilized as basic units<sup>6-9</sup>. Consequently, LIB development has been on the rise, especially for improving electrochemical performance with high energy and power densities and long life cycles.

Recently, considerable amount of research has been conducted on battery electrodes<sup>1, 6, 9, 10</sup> and electrolytes.<sup>11</sup> LIBs were found to have high energy density and power capability.<sup>12</sup> However, safety issues<sup>13</sup> regarding thermal stability and short-circuiting by the Lithium dendrites may be overlooked. A stable operation at high current density is much more significant in massive energy storage systems, so safety is a critical issue.

Electrodes and electrolytes are important in material selection as well as interfacial<sup>14</sup> and structural engineering due to LIB safety and stability. The safety issues are directly linked to the separator in the LIB system, because lithium cation transportation occurs in the separator and electrolyte complex. The separator plays a primary role in LIBs to prevent electrical short-circuiting between the cathode and anode. Additionally, it retains electrolytes in the porous matrix for the ion transportation medium<sup>15</sup>. The commercialized separators are mostly poly-olefins, such as polyethylene (PE), polypropylene (PP), polystyrene (PS), or their blend types (e.g., PE-PP, PS-PP, PET-PP, etc.). Those materials are advantageous for the mechanical and structural properties, electrochemical stability, and low cost production. Nevertheless, the commercialized separators have crucial weaknesses of low thermal stability<sup>16-19</sup>, inferior wettability<sup>18</sup>, and unfavourable complex structure<sup>20</sup> for ion transportation. Most poly-olefin separators begin to shrink above 120 °C<sup>19, 21</sup>, so they are likely to show thermal runaway, which causes critical failures such as fire explosion.

Here in, we introduce the anodic aluminum oxide (AAO) as a new material for a separator in LIBs. It provides a homogeneous interfacial reaction between the electrolyte and electrode, which can lead to long-term stability, high rate capacity, and increased safety. The AAO has an advantageous distinct nano-pore structure from its self-ordering ability, which can be enumerated as a highly ordered hexagonal pore array with extremely narrow pore size distribution<sup>22-24</sup>. Furthermore, the AAO has proper material properties like superior wettability, excellent thermal stability, chemical resistance, mechanical strength, and high porosity<sup>25, 26</sup>. With regard to the mechanical strength of the AAO, one of the suitable methods for suppressing Lithium dendrite growth is through physical and electrochemical stabilization. We believe that the AAO can exhibit better electrochemical properties than commercialized polyolefin separators.

The morphological and physical characteristics of the AAO separator were studied by utilizing a scanning electron microscopy (SEM). As-prepared AAO separator with perpendicular through-hole structure has an average pore size of 75 nm and thickness of 54 micron. Figure 1 shows that the fabricated AAO separator has (a) uniform pore size and hexagonal packed array, (b) completely open-hole structures of the barrier layer at the bottom, and (c) a straight channel with low AAO structure tortuosity. These properties can lead to moderate stripping and plating reactions on Li metal surface, and improve the electrochemical performance of the lithium ion battery due to the surface smoothing effects on the Li metal electrode<sup>27</sup>. Thus, this unique hexagonal pore array and cylindrical structure can provide significant advantages for LIBs.

Computer-aid simulation modelling was carried out to provide support for the AAO structure properties (Fig. 1 (d)). When the electric field is applied on the top and bottom of the AAO separator with the electrolyte system, the current pathways do not locally center while PP shows irregular concentration (Fig. S1, in the ESI). This means Li cations can transport at a flat rate and evenly exist at the interface between the separator pores and the electrode surfaces. It also causes uniform diffuse distribution at the interface where electrochemical redox reactions occur. Consequently, those effects can minimize charge transfer resistance in the LIBs due to relatively increased Li ion concentration at the electrode surface.<sup>26, 27</sup> The LIB capacity is advanced via the homogeneous interfacial reactions when the AAO separator is employed with significant structural features. Moreover, the structural advantages of the AAO imply that the Li metal can be utilized as an ideal anode (the highest theoretical capacity of 3400 mAh g<sup>-1</sup>) without any engineering to suppress the Li dendrite growth<sup>28-32</sup>.

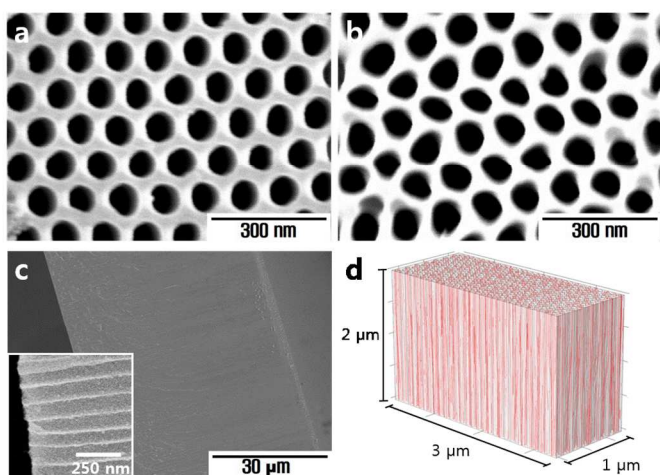


Figure 1. SEM characterization images of the AAO membrane (a) front, (b) bottom, and (c) cross-section. The modelling of the current passages in the porous AAO filled with organic electrolyte (1M LiPF<sub>6</sub> in EC/DMC in the weight ratio of 1/1) is simulated by finite element method (FEM) with COMSOL multiphysics. Red lines denote the current density in the AAO with the liquid electrolyte system.

Intrinsic properties of the anodic alumina are evaluated with regard to the important prerequisites for battery separators like porosity, electrolyte uptake, wettability, and thermal stability. The porosity and electrolyte uptake are very important parameters for the LIB separator, because these properties can determine the effectiveness of the ion transport medium. High pore densities per unit area can sufficiently hold the electrolyte, so the electrolyte is prevented from diffusing out quickly. The porosity and electrolyte uptake of the PP and AAO separator are defined by the weight change between dry and wet separators in the following equations:

$$\text{Porosity (\%)} = \left( \frac{W_f - W_i}{\rho_{liq} V_i} \right) \times 100 \quad [1]$$

where  $W_i$  and  $W_f$  denote the separator weights before and after immersion in n-butanol, respectively,  $\rho_{liq}$  is the n-butanol density, and  $V_i$  is the separator volume.

$$\text{Electrolyte uptake (\%)} = \frac{W_{wet} - W_{dry}}{W_{dry}} \times 100 \quad [2]$$

where  $W_{dry}$  and  $W_{wet}$  represent the weights of the membrane before and after the commercial liquid electrolyte absorption, which is 1M LiPF<sub>6</sub> in ethylene carbonate/dimethyl carbonate at a weight ratio of 1/1 (PANAX ETEC).

The porosity of the AAO membrane is calculated to be 67.4 %, which shows that the AAO separator has more porous structures than PP (about 55%<sup>33</sup>, Celgard 2500). Even though AAO has higher porosity, the Electrolyte uptakes of the PP membrane was 204.87 wt% and the AAO was 171.79 wt%. Therefore, the porous separators are fully wetted in the free volume of the pore structure when considering the density of the samples and organic electrolytes<sup>26</sup>.

To characterize the PP and AAO separator wettability (Fig. 2 (a)), the contact angles of each separator are measured with the same electrolyte used in uptake ability measurement (1M LiPF<sub>6</sub> in ethylene carbonate/dimethyl carbonate at a weight ratio of 1/1). As seen in Fig. 2 (b) and (c), the polyolefin separator has a contact angle of 72°, which is higher than that of AAO (23°). Thus, the AAO membrane can instantly infiltrate the organic electrolyte into free pore volumes due to the hydrophilicity, capillary force, and close polarity with liquid electrolyte<sup>26</sup>. This attractive intrinsic property of Al<sub>2</sub>O<sub>3</sub> also works well with previous reports that aluminum oxide can increase wettability, resulting in higher discharging capacity when using additional agents for the surface engineering of separator or gel polymer electrolytes<sup>34-36</sup>.

Thermal stability is also one of the major criteria in choosing a suitable candidate for the separator. To evaluate the thermal resistance, the AAO and PP membranes are placed in a convection oven at 120 °C for 30 min. Polypropylene based separators begin to shrink above 120 °C. Thermal shrinkage is calculated by the following equation:

$$\text{Shrinkage (\%)} = \frac{(A_i - A_f)}{A_i} \times 100 \quad [3]$$

where  $A_i$  and  $A_f$  represent the areas before and after the membrane thermal shrinkage test, respectively. The dimensional PP change is about 23 % (Fig 2 (d) and (e)), but the AAO separator does not show any contractions (Fig 2 (f) and (g)). The PP separator did not recover to the initial structure after cooling at room temperature. Therefore, the AAO is stable for LIB operation at wide temperature ranges.

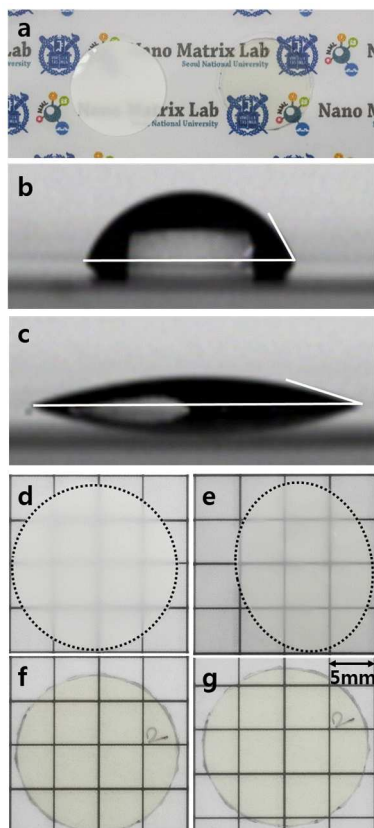


Figure 2. (a) Optical photographs of the 19 mm diameter PP and AAO separator as the final products. (b, c) The contact angles of the PP membrane (72°) and the AAO (23°). Before and after heat instability tests of PP (d, e) and AAO (f, g). The PP separator displayed dimensional shrinkage about 23 % while the AAO had no changes.

As displayed in Figure 3 (a), the AAO separator with liquid electrolyte has a higher conductivity of  $2.196 \text{ mS cm}^{-1}$  than of the PP separator ( $0.701 \text{ mS cm}^{-1}$ ). The better ionic conductive properties mainly come from the high porosity and uniform distribution of Li ions. The ordered porous structure can retain organic electrolytes sufficiently as an important prerequisite for the efficient Li ion diffusion. We attempt to introduce the AAO separator with outstanding properties into the energy storage system and the electrochemical half-cells are evaluated by assembling Lithium Iron Phosphate ( $\text{LiFePO}_4$ , LFP) electrodes into working electrode. The Li metal is used as a reference and the counter electrode is assembled into coin-cells. From the AC impedance data (Fig 3 (b)), the AAO separator has smaller charge transfer resistance ( $R_{ct}$ ) of  $133.73 \Omega$  and larger ionic conductivity ( $\sigma$ ) of  $1.804 \times 10^{-2} \text{ mS cm}^{-1}$  than the PP membrane cell ( $R_{ct}$  and  $\sigma$  are  $188.41 \Omega$  and  $1.000 \times 10^{-2} \text{ mS cm}^{-1}$ , respectively). In order to further investigate the electrochemical

characteristics with different separators, the cycling performance test is conducted as it is seen in Fig. 3 (c). The cycling properties and coulombic efficiency are inspected at a high current rate of 5 C ( $1.325 \text{ mA cm}^{-1}$ ) over 120 cycles. After 50 cycles of charging and discharging, the PP cell capacity rapidly decreased while the AAO was stable. The discharge capacity percentage difference between the first cycle at 5 C ( $10^{\text{th}}$  and  $130^{\text{th}}$  cycle in Fig. S2) and the  $120^{\text{th}}$  cycle of the PP and AAO batteries are 31.80 % (varied from  $68.72 \text{ mAh g}^{-1}$  to  $46.87 \text{ mAh g}^{-1}$ ) and 17.34 % (from  $83.41 \text{ mAh g}^{-1}$  to  $68.94 \text{ mAh g}^{-1}$ ), respectively. The coulombic efficiency of the AAO and PP cell is about 100 %.

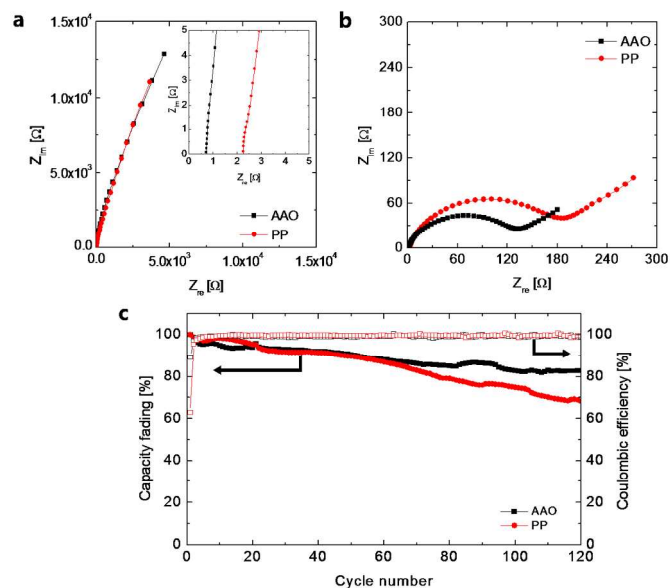


Figure 3. (a) The Nyquist plot of the half cells with the PP and AAO separator for the ionic conductivities. The AAO employed cell performs better over high frequency ranges (inset). (b) Internal resistance characterized for the PP and AAO half cell (sandwiched between Li metal and Lithium Iron Phosphate, LFP) by the AC impedance analyzer. (c) The discharging capacity variation and coulombic efficiency of the AAO and PP cells.

Moreover, the rate capability, capacity retention, and the AC impedance tests are studied with a full cell of LFP and Lithium titanate ( $\text{Li}_4\text{Ti}_5\text{O}_{12}$ , LTO) as cathode and anode, respectively. The AC impedance analysis was done before and after the rate behaviour test to determine the ionic conductivity change. As shown on the Nyquist plot (Fig.4 a), the AAO and PP separator-battery has  $4.421 \times 10^{-2} \text{ mS cm}^{-1}$  and  $1.469 \times 10^{-2} \text{ mS cm}^{-1}$ , respectively. During the rate capability examination (Fig 4 b), the current rate increased from 0.2 C to 10 C, with each step reflecting 5 cycles. At the beginning of 0.2 C, the AAO shows a higher capacity with  $71.4 \text{ mAh g}^{-1}$  rather than  $66.4 \text{ mAh g}^{-1}$  given by PP. The difference was observed at the current density of 10 C where the AAO is three times bigger ( $20.13 \text{ mAh g}^{-1}$ ) than the PP capacity ( $6.52 \text{ mAh g}^{-1}$ ). The Li ion diffusion in the AAO is more efficient than in PP. At the end of the rate capability test, the AAO and PP cells recover 82.9 % and 80.8 % of the initial capacity, respectively. This means that the electrodes in the AAO separator cell were less damaged than the electrodes in the PP-cell. In consideration of our simulation model, regularly-ordered

close-packed array of nanopores allows even current distribution on the electrode surface, thus AAO used electrochemical cells can perform with higher capacity and greater rate capabilities than PP membrane employed batteries. Once again, it is confirmed that regular pore arrays and cylindrical morphologies are favorable and prerequisites for high current charging-discharging LIBs. This result matches the Nyquist plot data in Figure 4 (a). After the rate behaviour experiment, the AC impedance measurement determines the changes in ionic conductivity. The AAO separator employed battery has  $3.519 \times 10^{-2} \text{ mS cm}^{-1}$ , which shows a slightly reduced, but still much higher value in comparison with the PP separator used.

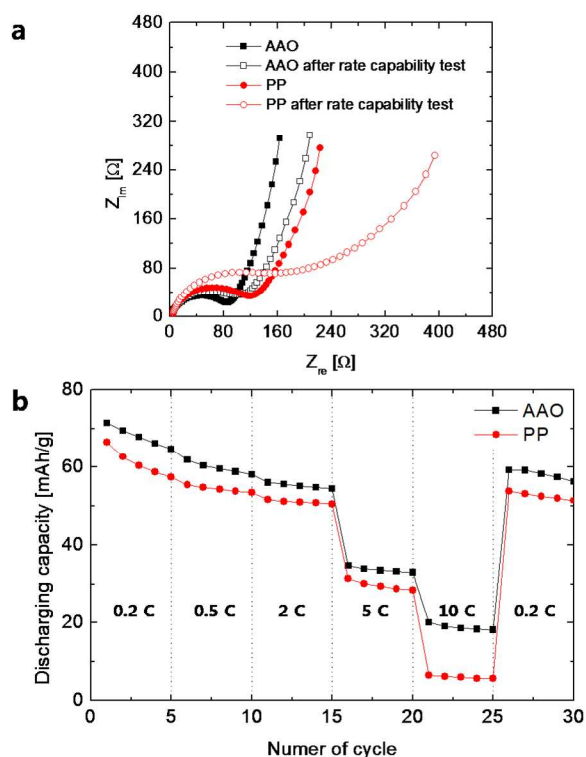


Figure 4. (a) The Nyquist plot shows before and after current rate behavior test of the PP and AAO full cell. (b) The rate capability results of the AAO and PP membrane cells are also provided.

## Conclusions

In summary, we introduced an ideal AAO separator structure for the Lithium-Ion Battery system. The electrochemical performances of lithium ion batteries tend to depend on the structural properties of the separator. The porous framework and vertically straight channels with extremely low tortuosity allow for improved battery efficiency, better conductivity, higher discharging capacity, and superior rate retention capability. Through electrochemical experiments and computer aid simulation, highly ordered hexagonal pore arrays were found to effectively migrate lithium ions and evenly distribute the current density. This can effectively suppress lithium dendrite growth on

the lithium metal surface. The Li-metal is an ideal anode material due to these powerful capabilities.

## Experimental details

The AAO separators were fabricated by a two-step anodization method as shown in Fig. S3. Highly pure aluminum (Al) plates (99.999 %, 0.55mm thick, purchased from Good fellow, Ltd.) were prepared as 2 cm X 7.5 cm specimens then degreased, which cleaned the Al surface with acetone and ethanol. Afterwards, the specimens were electropolished at constant 20 V in 0 °C in a perchloric acid and ethanol mixture (1:4, v/v) for 6 to 8 min to make smooth surfaces and remove impurities like native oxides and dust. When the Al samples had "mirror-like" surfaces, anodization was carried out in 0.3 M oxalic acid solution by applying 40 V at 15 °C for 12 hours. Before conducting the 2<sup>nd</sup> anodization step, the alumina layer was etched away by chromium (VI) oxide solution immersion at 65 °C for 5 hours. The anodic aluminum oxide layer with highly ordered pore array was grown along the pretextured nanopits during the second anodization step. Furthermore, the aluminum substrate was removed by immersing in a mixed solution of 0.3 M  $\text{CuCl}_2$  and hydrochloric acid at a volume ratio of 1:1. The bottom AAO barrier layer was removed by floating on the 5 wt%  $\text{H}_3\text{PO}_4$  solution surface for 60 min at the final stage. To evaluate the structural and morphological features, manufactured samples were characterized by a scanning electron microscopy (Hitachi, S-4800).

To characterize the electrochemical properties of the AAO separator, CR-2032 coin cells were assembled for specific purposes. Stainless steel disks were used as electrodes and liquid electrolytes (1 M  $\text{LiPF}_6$  in EC/DMC, the volume ratio of 1/1) for the ionic conductivity measurements. The AC impedance spectroscopy was used (CHI660E, CH Instrument) from 1 HZ to 1 MHz at room temperature with 5 mV amplitude to calculate the ionic conductivity ( $\sigma$ ) in equation [4].

$$\text{Ionic conductivity } (\sigma) = \frac{L}{R_b A} \quad [4]$$

where L is the thickness of the separator, A is the contact area in between the separator and the stainless steel (SUS) electrode, and  $R_b$  is the bulk resistance.

The cell resistance was evaluated *via* an AC impedance test conducted by electrochemical cells and composed of  $\text{LiFePO}_4$  (LFP) cathode, drenched separator with liquid electrolyte, and 150  $\mu\text{m}$  thick Li foil. The cell assembly was performed under an argon atmosphere and the cathode was prepared by coating a Lithium Iron Phosphate (LFP,  $\text{LiFePO}_4$ , MTI Korea) slurry containing PVdF (Mw. 540000, Aldrich) binder and Super P (Timcal) as a conducting agent (in a weight ratio of 8:1:1) in N-Methyl-2-pyrrolidone (NMP, Daejung chemical). The slurry was applied on the aluminum substrate (15 $\mu\text{m}$  thick) using a Meyer rod.

The full cell consists of the LFP cathode, PP or AAO membrane with liquid electrolyte, and Lithium titanate ( $\text{Li}_4\text{Ti}_5\text{O}_{12}$ , LTO, MTI Korea) anode. The LTO anode was fabricated by coating 9  $\mu\text{m}$

thick copper foil using Mayer rod. The slurry was composed of LTO, PVdF, and Super P in a 8:1:1 (w/w/w) ratio. Each slurry was mixed with homogenizer (AR 100, Thinky mixer) at 2000 rpm for 5 min. The manufactured full cells were subjected to analyze capacity, cycling test, and rate capability by investigating the charging-discharging characteristics in a battery cycler system (WBCS 3000L, WonATech).

### Acknowledgements

This work was supported by Basic Research Program (2011–0018113) of National Research Foundation (NRF) of Korea, Center for Advanced Soft Electronics as Global Frontier Research Program (2013M3A6A5073177) of the Ministry of Science, ICT and Future Planning of Korea and Railroad Technology Research Program (13RTRP-C068308-01) of Ministry of Land, Infrastructure and Transport of Korea.

### Notes and references

<sup>a</sup> Program in Nano Science and Technology, Graduate School of Convergence Science and Technology, Seoul National University Seoul 151-744, Republic of Korea. E-mail: younskim@snu.ac.kr

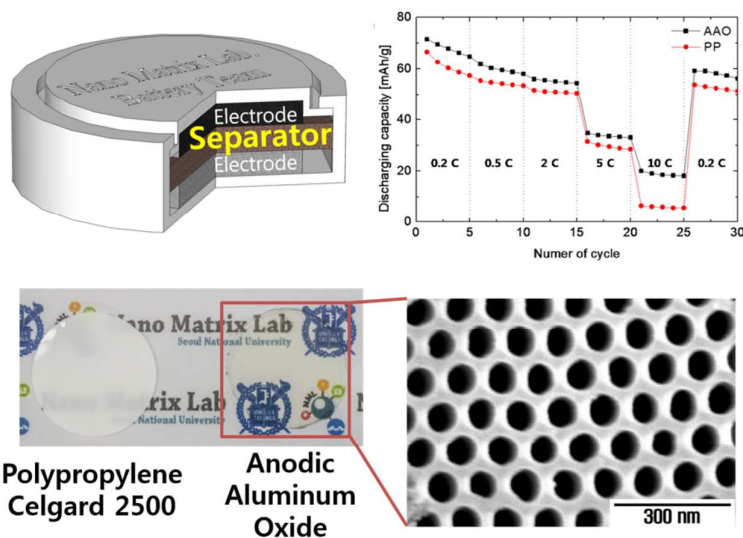
<sup>b</sup> Korea JCC CO. LTD. R&D Center 1163, Chungcheong-daero, Bugi-myeon, Cheongwon-gun, Chungcheongbuk-do 363-922, Republic of Korea

<sup>c</sup> Advanced Institutes of Convergence Technology, 864-1 Iui-dong, Yeongtong-gu, Suwon-si, Gyeonggi-do 443-270, Republic of Korea

† Electronic Supplementary Information (ESI) available. See DOI: 10.1039/c000000x/

- J. M. Tarascon and M. Armand, *Nature*, 2001, **414**, 359-367.
- Y. S. Zhu, F. X. Wang, L. L. Liu, S. Y. Xiao, Y. Q. Yang and Y. P. Wu, *Sci Rep-Uk*, 2013, **3**.
- X. S. Huang, D. Bahroloomi and X. R. Xiao, *J Solid State Electr*, 2014, **18**, 133-139.
- J. Wang, Z. Hu, X. Yin, Y. Li, H. Huo, J. Zhou and L. Li, *Electrochim Acta*, 2015, **159**, 61-65.
- B. Scrosati, J. Hassoun and Y. K. Sun, *Energ Environ Sci*, 2011, **4**, 3287-3295.
- S. Goriparti, E. Miele, F. De Angelis, E. Di Fabrizio, R. P. Zaccaria and C. Capiglia, *J Power Sources*, 2014, **257**, 421-443.
- P. Arora and Z. M. Zhang, *Chem Rev*, 2004, **104**, 4419-4462.
- J. Y. Kim, Y. Lee and D. Y. Lim, *Electrochim Acta*, 2009, **54**, 3714-3719.
- N. Nitta and G. Yushin, *Part Part Syst Char*, 2014, **31**, 317-336.
- Y. He, X. Q. Yu, Y. H. Wang, H. Li and X. J. Huang, *Adv Mater*, 2011, **23**, 4938-4941.
- J. W. Fergus, *J Power Sources*, 2010, **195**, 4554-4569.
- H. Gwon, J. Hong, H. Kim, D.H. Seo, S. Jeon and K. Kang, *Energ Environ Sci*, 2014, **7**, 538-551.
- R. Bouchet, *Nat Nanotechnol*, 2014, **9**, 572-573.
- M. Kirchofer, J. von Zamory, E. Paillard and S. Passerini, *Int J Mol Sci*, 2014, **15**, 14868-14890.
- S. S. Zhang, *J Power Sources*, 2007, **164**, 351-364.
- N. S. Choi, Z. H. Chen, S. A. Freunberger, X. L. Ji, Y. K. Sun, K. Amine, G. Yushin, L. F. Nazar, J. Cho and P. G. Bruce, *Angew. Chem., Int. Ed.*, 2012, **51**, 9994-10024.
- T. H. Cho, M. Tanaka, H. Onishi, Y. Kondo, T. Nakamura, H. Yamazaki, S. Tanase and T. Sakai, *J Power Sources*, 2008, **181**, 155-160.
- J. Lee, C. L. Lee, K. Park and I. D. Kim, *J Power Sources*, 2014, **248**, 1211-1217.
- Y. Ko, H. Yoo and J. Kim, *Rsc Adv*, 2014, **4**, 19229-19233.
- G. Y. Gor, J. Cannarella, J. H. Prevost and C. B. Arnold, *J Electrochem Soc*, 2014, **161**, F3065-F3071.
- K. J. Kim, H. K. Kwon, M. S. Park, T. Yim, J. S. Yu and Y. J. Kim, *Phys Chem Chem Phys*, 2014, **16**, 9337-9343.
- H. Masuda and K. Fukuda, *Science*, 1995, **268**, 1466-1468.
- K. Nielsch, F. Muller, A. P. Li and U. Gosele, *Adv Mater*, 2000, **12**, 582-586.
- R. Krishnan and C. V. Thompson, *Adv Mater*, 2007, **19**, 988-+.
- A. Mozalev, S. Magaino and H. Imai, *Electrochim Acta*, 2001, **46**, 2825-2834.
- J. J. Chen, S. Q. Wang, L. X. Ding, Y. B. Jiang and H. H. Wang, *J Membrane Sci*, 2014, **461**, 22-27.
- S. J. Kang, T. Mori, J. Suk, D. W. Kim, Y. K. Kang, W. Wilcke and H. C. Kim, *J Mater Chem A*, 2014, **2**, 9970-9974.
- K. Murata, S. Izuchi and Y. Yoshihisa, *Electrochim Acta*, 2000, **45**, 1501-1508.
- R. Mogi, M. Inaba, S. K. Jeong, Y. Iriyama, T. Abe and Z. Ogumi, *J Electrochem Soc*, 2002, **149**, A1578-A1583.
- Y. Y. Lu, S. K. Das, S. S. Moganty and L. A. Archer, *Adv Mater*, 2012, **24**, 4430-4435.
- F. Ding, W. Xu, G. L. Graff, J. Zhang, M. L. Sushko, X. L. Chen, Y. Y. Shao, M. H. Engelhard, Z. M. Nie, J. Xiao, X. J. Liu, P. V. Sushko, J. Liu and J. G. Zhang, *J Am Chem Soc*, 2013, **135**, 4450-4456.
- S. H. Kim, K. H. Choi, S. J. Cho, E. H. Kil and S. Y. Lee, *J Mater Chem A*, 2013, **1**, 4949-4955.
- Q. Xu, Q. Kong, Z. Liu, J. Zhang, X. Wang, R. Liu, L. Yue and G. Cui, *Rsc Adv*, 2014, **4**, 7845-7850.
- D. Takemura, S. Aihara, K. Hamano, M. Kise, T. Nishimura, H. Urushibata and H. Yoshiyasu, *J Power Sources*, 2005, **146**, 779-783.
- K. J. Kim, J. H. Kim, M. S. Park, H. K. Kwon, H. Kim and Y. J. Kim, *J Power Sources*, 2012, **198**, 298-302.
- C. Z. Man, P. Jiang, K. W. Wong, Y. Zhao, C. Y. Tang, M. K. Fan, W. M. Lau, J. Mei, S. M. Li, H. Liu and D. Hui, *J Mater Chem A*, 2014, **2**, 11980-11986.

## Enhanced Electrochemical Capabilities of Lithium Ion Batteries by Structurally Ideal Anodic Aluminum Oxide Separator



Anodic aluminum oxide (AAO) membrane is introduced as a structurally ideal separator for Lithium ion batteries (LIBs), those advantageous nano-porous properties have strong potential for lithium metal utilization as an ideal anode due to even current distribution. Furthermore, electrochemical performance of AAO separator exhibit better ionic conductivity, higher discharging capacity, and low capacity fading at high current densities with compared to commercial polypropylene separator.